minerals

MDPI

Article

Synthesis of Hydroxy-Sodalite/Cancrinite Zeolites from Calcite-Bearing Kaolin for the Removal of Heavy Metal Ions in Aqueous Media

Muayad Esaifan [1,2,*], Laurence N. Warr [2], Georg Grathoff [2], Tammo Meyer [2], Maria-Theresia Schafmeister [2], Angela Kruth [3] and Holger Testrich [3]

1 Department of Chemistry, Faculty of Arts and Sciences, University of Petra, Amman 11196, Jordan
2 Institute of Geography and Geology, University of Greifswald, 17487 Greifswald, Germany
3 Leibniz Institute for Plasma Science and Technology (INP), 17487 Greifswald, Germany
* Correspondence: muayad.esaifan@uop.edu.jo

Received: 5 July 2019; Accepted: 10 August 2019; Published: 13 August 2019

Abstract: A hydroxy-sodalite/cancrinite zeolite composite was synthesized from low-grade calcite-bearing kaolin by hydrothermal alkali-activation method at 160 °C for 6 h. The effect of calcite addition on the formation of the hydroxy-sodalite/cancrinite composite was investigated using artificial mixtures. The chemical composition and crystal morphology of the synthesized zeolite composite were characterized by X-ray powder diffraction, infrared spectroscopy, scanning electron microscopy, and N_2 adsorption/desorption analyses. The average specific surface area is around 17–20 $m^2 \cdot g^{-1}$, whereas the average pore size lies in the mesoporous range (19–21 nm). The synthesized zeolite composite was used as an adsorbent for the removal of heavy metals in aqueous solutions. Batch experiments were employed to study the influence of adsorbent dosage on heavy metal removal efficiency. Results demonstrate the effective removal of significant quantities of Cu, Pb, Ni, and Zn from aqueous media. A comparative study of synthesized hydroxy-sodalite and hydroxy-sodalite/cancrinite composites revealed the latter was 16–24% more efficient at removing heavy metals from water. The order of metal uptake efficiency for these zeolites was determined to be Pb > Cu > Zn > Ni. These results indicate that zeolite composites synthesized from natural calcite-bearing kaolin materials could represent effective and low-cost adsorbents for heavy metal removal using water treatment devices in regions of water shortage.

Keywords: natural clay; water purification; zeolite; minerals; pollution

1. Introduction

The use of treated wastewater has become a potential solution to alleviate seasonal water shortages caused by drought or problems of infra structure in many dry countries and is particularly important for use in irrigation, toilet flushing, and firefighting [1,2]. Local water treatment systems rely on the removal of heavy metals and organic pollutants largely by chemical adsorption. This is often achieved by complicated and expensive methods such as ion exchange, membrane filtration, and electrochemical processes [3,4]. Heavy metals are considered the most hazardous groundwater pollutants and originate from industrial activities as well as the overuse of fertilizers in agriculture. Among these heavy metals, Pb, Cu, Zn, and Ni are considered to be the most studied and problematic of water pollutants [5,6]. According to World Health Organization standards (WHO), the permissible limits of Pb, Cu, Zn, and Ni in drinking water are 0.01, 2.0, 3.0, and 0.02 ppm, respectively [7]. The principal challenges of effective treatment are to overcome the high costs involved and deal with the large volumes of water that fluctuate significantly in quality [4,8].

Over the last years, a number of investigations were conducted to test the use of natural zeolites as low-cost adsorbents for the removal of heavy metals [9], salts [10], and ammonium ions [11]. Zeolite-based adsorbents have a unique crystalline microporous structure and high metal-binding capacity [12,13], and in some cases are suitable for detoxifying the body by consumption [14]. These minerals are characterized by a notably uniform pore structure with a molecular dimension <0.13 nm formed between tetrahedrally coordinated Si^{4+} and Al^{3+} that are connected via oxygen atoms [15]. Due to the limited availability of pure natural zeolites, researchers have turned towards synthetic zeolites for adsorbent purposes [16–18]. Zeolites are most commonly synthesized by hydrothermal alkali-activation of aluminosilicate materials at appropriate temperatures (100–1000 °C) and pressures (1~100 MPa) in high-pressure autoclaves [19–21].

The most used natural aluminosilicate for zeolites synthesis is kaolinite and its thermally activated phase (metakaolinite), which constitute highly reactive and pure precursor materials [22,23]. Kaolinite and metakaolinite based zeolite synthesis involves mixing the solid precursor with sodium hydroxide and sodium silicate as the alkaline activating solution [24]. Important synthesis parameters are (i) the SiO_2/Al_2O_3 molar ratio, (ii) the alkalinity of the reacting solution, (iii) the curing temperature, and (iv) the reaction time. Among these parameters, the alkalinity is known to be a key factor that determines the type of synthesized zeolite [24]. In addition to kaolinite/metakaolinite materials, industrial waste such as coal fly ash has also been used to produce Na-A, Na-X, and Na-P1 zeolites [25–27].

As an example of the alkali-activation of kaolinite, it has been reported that hydroxy-sodalite is produced when using NaOH at a molarity of 10 or higher [28]. In contrast, zeolite Na-P1, zeolite LTA, sodalite, and analcime result when the concentration of NaOH in the reaction mixture is lower than a molarity of 4 [24,29]. Different cost-effective binary alkaline systems of low causticity have also been developed for the alkali-activation of kaolinite [22,30]. Esaifan et al. [22] reported the formation of a kaliophilite zeolite by reacting kaolinite with calcium hydroxide/potassium carbonate ($Ca(OH)_2/K_2CO_3$) as the alkaline activating mixture. Shaqour et al. [30] also synthesized a cancrinite-type zeolite by activating kaolinite with a calcium hydroxide/sodium carbonate ($Ca(OH)_2/Na_2CO_3$) alkaline mixture.

The high adsorption capacity of synthetic hydroxy-sodalite and cancrinite zeolites has led a number of researchers to propose them as potential adsorbents for heavy metal removal from contaminated water [16,31,32]. Sodalite and cancrinite zeolites have the common chemical formula of $Na_6(Al_6Si_6O_{24})\cdot 2X\cdot nH_2O$ but vary in their crystal structure. Sodalite has a cubic crystal structure formed by the stacking of 14-hedra composed of eight six-membered rings (β cage: 6.6 Å) with alternating AlO_4 and SiO_4 tetrahedra, and six four-membered rings (ε cage: 2.2 Å). In contrast, cancrinite has a hexagonal crystal structure formed by the stacking of 11-hedra of five 12-membered rings (β cage: 6.2 Å) and six four-membered rings. The β cages contain large continuous channels for extra-framework cations (Na^+, Ca^{2+}), anions (CO_3^{2-}, OH^-), and H_2O molecules whereas the ε cage hold $[Na\cdot H_2O^+]$ clusters. The presence of these continuous channels allows NaOH or $CaCO_3$ to replace X in the above formula to form hydroxy-sodalite and cancrinite, respectively [33–35]. Xu et al. [35] studied the effect of calcium addition on the transformation of sodalite to cancrinite during Bayer digestion and found it accelerated both the formation of cancrinite and the transformation of sodalite to cancrinite.

Composite adsorbent materials are currently of considerable interest due to their cost-effective treatment of metal-contaminated wastewater [36–39]. Ahmad and Mirza [37] prepared a bionanocomposite synthesized from Alginate-Au-Mica with a high effective adsorption capacity for removing Pb^{2+} and Cu^{2+} from wastewater (225.0 and 169.8 mg g^{-1}, respectively). Ahmad and Mirza [36] also showed that a chitosan-iron oxide nanocomposite can be used to effectively remove Pb^{2+} and Cd^{2+} from aqueous solutions, with similarly high maximum adsorption capacities (214.9 and 204.3 mg·g^{-1}, for Pb^{2+} and Cd^{2+}).

In light of the above development, the aim of this work was to synthesize a low-cost composite adsorbent comprised of hydroxy-sodalite/cancrinite by hydrothermal and alkali-activation treatment of a widely available, cost-effective, calcite-bearing kaolin material. The effect of accessory calcite on the

synthesis of zeolite from powdered kaolin rock was investigated in terms of the quality of the resulting adsorbent. The chemical and morphological structure of the synthesized adsorbent was studied by X-ray diffraction (XRD), scanning electron microscopy (SEM), and N_2 adsorption/desorption isotherms. The synthesized zeolite composite was then tested as an adsorbent to remove Pb^{2+}, Cu^{2+}, Zn^{2+}, and Ni^{2+} ions from aqueous media. The influence of the adsorbent dosage on the efficiency of removing heavy metals was also studied on the basis of further batch experiments. Based on these results, we highlight the usefulness of developing, low cost, water-purifying composite adsorbents synthesized from regionally available materials.

2. Materials and Methods

2.1. Raw Material

The natural calcite-bearing kaolin used in this study as a solid precursor was collected from the Batn El-Ghoul deposit, Jordan. According to the Ministry of Energy and Mineral Resources of Jordan, the estimated reserve of this deposit is about 2.2 billion tons [40]. Its clay mineralogy was studied by Khoury and El-Sakka [41] who classified it as low-grade kaolin clay due to the presence of calcite (5–10%) and iron oxide (2–6%). The amount of kaolinite in this deposit was estimated by Esaifan et al. [28] to be about 68% based on thermogravimetric analysis. According to XRF analysis, calcite-bearing kaolin contains a CaO content of 5.3%, which is equivalent to 9.5% $CaCO_3$. This low grade kaolin is therefore not a prime choice for use in the paper or ceramic industry. China clay in the form of almost pure kaolinite was also used for comparison, which was supplied by Carl Roth chemicals, Germany. The chemical composition of the two clay samples, determined by X-ray fluorescence analyses following the procedure of described by Dietel et al. [42], is given in Table 1.

Table 1. Chemical composition (wt. %) of the raw materials based on X-ray fluorescence analyses. L.O.I—lost-on-ignition.

Sample	Weight Percentage (%)										
	Al_2O_3	SiO_2	CaO	Fe_2O_3	K_2O	MgO	TiO_2	Na_2O	L.O.I	Total	Si/Al
China Clay	39.4	48.0	-	0.5	1.0	-	0.1	0.1	13.6	102.7	1.1
Calcite bearing kaolin	25.2	53.3	5.3	2.5	1.3	0.2	0.4	0.2	11.1	99.5	1.9

2.2. Synthesis of the Hydroxy-Sodalite/Cancrinite Zeolite Composite

Zeolite composite was synthesized by hydrothermal and alkali-activation treatment at 160 °C for 6 h. A set of high-pressure and high-temperature, Teflon-lined, stainless steel vessels were used for the hydrothermal synthesis. The alkaline activator was prepared by dissolving NaOH pellets (Carl Roth, 99.0%) in deionized water in a capped plastic bottle. Afterward, the synthesized zeolite was dried at 105 °C for 24 h, then crushed using a Fritsch planetary micro-mill pulverisette 7 and sieved to ≤40 μm [28].

Three zeolite specimens were prepared using specific mass percentages of NaOH, water, clay, and calcite as described in Table 2. The first specimen (labeled as China Clay + NaOH) was prepared by mixing NaOH, water and China clay to prepare the hydroxy-sodalite zeolite. The second specimen (labeled as China Clay + calcite + NaOH) was prepared by mixing NaOH, water, China clay, and calcite ($CaCO_3$) to prepare hydroxy-sodalite/cancrinite zeolites. This was used as a reference mixture for comparison. The third specimen (labeled as Calcite-bearing kaolin + NaOH) was prepared by mixing NaOH, water and the Jordanian calcite-bearing kaolin.

Table 2. Specimen mix composition used in hydrothermal alkali-activation experiments.

Specimen	Unit	Mix Composition				Total
		Clay	NaOH	Water	Calcite	
China Clay + NaOH	(fraction)	100	50	50	0	200
	(mass %)	0.50	0.25	0.25	0.00	1.0
	(grams)	50	25	25	0	100
China Clay + calcite + NaOH	(fraction)	100	50	50	8	208
	(mass %)	0.48	0.24	0.24	0.04	1.0
	(grams)	48	24	24	4	100
Calcite-bearing kaolin + NaOH	(fraction)	90.5	50.0	50.0	9.5 [a]	200
	(mass %)	0.45	0.25	0.25	0.05 [a]	1.0
	(grams)	45.25	25.00	25.00	4.75 [a]	100

[a]: calcite contained in natural sample and estimated by XRF analysis in Section 2.1.

2.3. Characterization of the Synthesized Zeolites

XRD diffraction patterns were obtained using a D8 Advance diffractometer (Bruker Corporation, Billerica, USA) with Co Kα radiation, operated at 30 mA and 40 kV and equipped with a LynxEye 1-dimensional detector. The diffraction patterns of the synthesized zeolites were measured over the 2θ range of 5–80° (scan speed of 2°/min and step scan size of 0.01). Mineral patterns were matched using the powder diffraction pattern database (ICDD-PDF-2 release) in combination with the Bruker Diffraction Eva software (Version 14, Bruker Corporation, Billerica, USA). Zeolite morphology was investigated by placing the fine powder on carbon-coated samples and imaged using an EVO MA10 SEM (CARL ZEISS AG, Oberkochen, Germany) coupled with an EDAX TEAM energy-dispersive X-ray spectroscopy (EDS) system. The samples were imaged under a vacuum pressure of 1×10^{-6} Pa and using a 15 kV accelerating voltage. Infrared spectra were obtained by using a Fourier transform infrared (FTIR)-attenuated total reflection (ATR) spectrometer (VERTX 80V, Bruker Corporation, Billerica, USA), coupled with an attenuated total reflectance diamond crystal unit. Spectra were collected from 4000 to 650 cm^{-1} at a resolution of 2 cm^{-1} and averaged over 32 scans. Specific surface areas and pore size properties of the synthesized zeolites were determined by an N_2 adsorption-desorption analyzer (NOVA, Quantachrome Instruments, Boynton Beach, FL, USA). Samples were outgassed using nitrogen (99.99%) for 3 h at 350 °C. The adsorption/desorption data were treated using standard multi-point Brunauer-Emmett-Teller (BET), Dubinin-Radushkevich (DR) and Barrett-Joyner-Halenda (BJH) models [27,43].

2.4. Synthetic Wastewater Preparation

Single metal aqueous solutions were prepared by diluting analytical grade Pb^{2+}, Cu^{2+}, Zn^{2+}, and Ni^{2+} 1000 ppm standard solutions supplied by Carl Roth chemicals in distilled water to obtain metal concentrations each with 100 ppm. The pH of the solutions was adjusted to be 5.5 ± 0.5 using 0.1 M HNO_3 or 0.1 M NaOH, to avoid heavy metal precipitation [44].

2.5. Heavy Metal Uptake Experiments

In order to study the effect of adsorbent (synthesized zeolites) dosage on the heavy metal removal efficiency, batch experiments were conducted with 100 mL of 100 ppm metal ion concentration placed in 250 mL conical flasks. The synthesized zeolites were dosed at 0.1, 0.2, 0.3, 0.4, 0.6, 0.8, 1.0, 1.2, and 1.5 g. The solutions were shaken for 2 h at room temperature (25 ± 0.1 °C) using a GFL 3040 shaker (Gesellschaft für Labortechnik mbH, Burgwedel, Germany) and then filtered using Whatman filter paper (No. 42) with a particle retention of 2.5 µm. Metal ion concentrations in the filtrate were analyzed using an Analytik Jena Contra 300 atomic absorption spectrometer (Analytik Jena, Jena, Germany).

The adsorbent removal efficiency (%) was calculated using Equation (1).

$$\text{Removal efficiency (\%)} = (C_i - C_f/C_i) \times 100, \quad (1)$$

where C_i (ppm) is the initial concentration of heavy metal ions and C_i (ppm) is the final concentration of metal ions.

3. Results and Discussion

3.1. Characterization of the Synthesized Zeolite

The XRD patterns of china clay and its hydrothermal alkali-activation products show the characteristic reflections of kaolinite (Figure 1a) completely disappeared after treatment to form a crystalline hydroxy-sodalite zeolite phase (Figure 1b). The addition of calcite to the China clay led to extra reflections upon alkali-activation attributable to cancrinite (Figure 1c). The XRD patterns of the natural calcite-bearing kaolin sample show kaolinite as the major component and quartz and calcite as impurities (Figure 2a). Two features were observed following hydrothermal alkali-activation of the calcite-bearing kaolin (Figure 2b); (1) the complete disappearance of kaolinite and a significant decrease in the intensity of quartz reflections. These features imply the complete dissolution of kaolinite and partial dissolution of quartz to release free species of Al and Si. (2) The appearance of XRD reflections assigned to cancrinite and hydroxy-sodalite indicates the crystallization of released Al and Si species and reaction with calcite to form cancrinite (Equation (2)). Once the calcite was consumed, hydroxy-sodalite started to crystallize (Equation (3)), similar to that observed in the hydrothermal alkali-activation of the China clay and calcite mixture (Figure 1c). These reactions can be expressed as:

$$3Al_2O_3{\cdot}2SiO_2{\cdot}H_2O + CaCO_3 + 6NaOH \rightarrow Na_6Al_6Si_6O_{24}(CaCO_3){\cdot}2H_2O + 4H_2O, \quad (2)$$

$$3Al_2O_3{\cdot}2SiO_2{\cdot}H_2O + 8NaOH \rightarrow Na_8Al_6Si_6O_{24}(OH)_2{\cdot}4H_2O + 2H_2O. \quad (3)$$

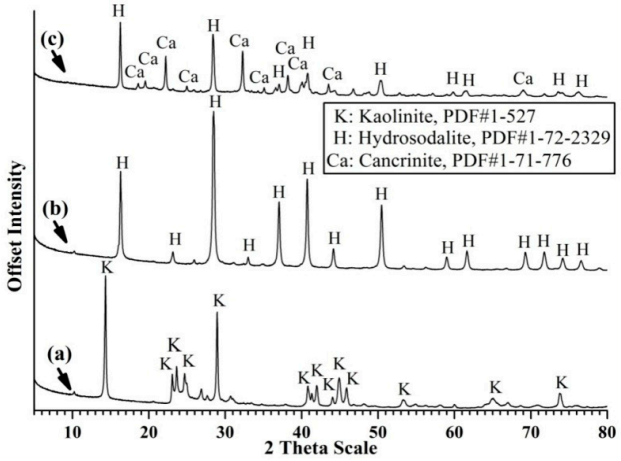

Figure 1. The X-ray diffraction (XRD) patterns of (**a**) raw China clay, the hydrothermal alkali-activation products; (**b**) China clay and (**c**) China clay and calcite.

SEM images of the hydrothermal alkali-activation product of China clay (Figure 3a) are characterized by homogenous pseudohexagonal crystals of hydroxy-sodalite zeolite, similar to previously published studies [45]. The presence of calcite during the hydrothermal alkali-activation of China clay gave rise to additional long hexagonal needles (Figure 3b) characteristic of cancrinite [46]. Similar morphologies are observed following hydrothermal alkali-activation of the calcite-bearing kaolin (Figure 3c). This can be explained by the dissolution of calcite present in the calcite-bearing kaolin, detectable in the XRD pattern (Figure 2).

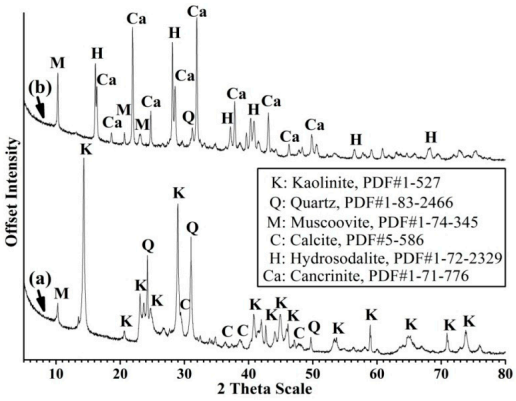

Figure 2. XRD patterns of (**a**) raw calcite-bearing kaolin and (**b**) its hydrothermal alkali-activation product.

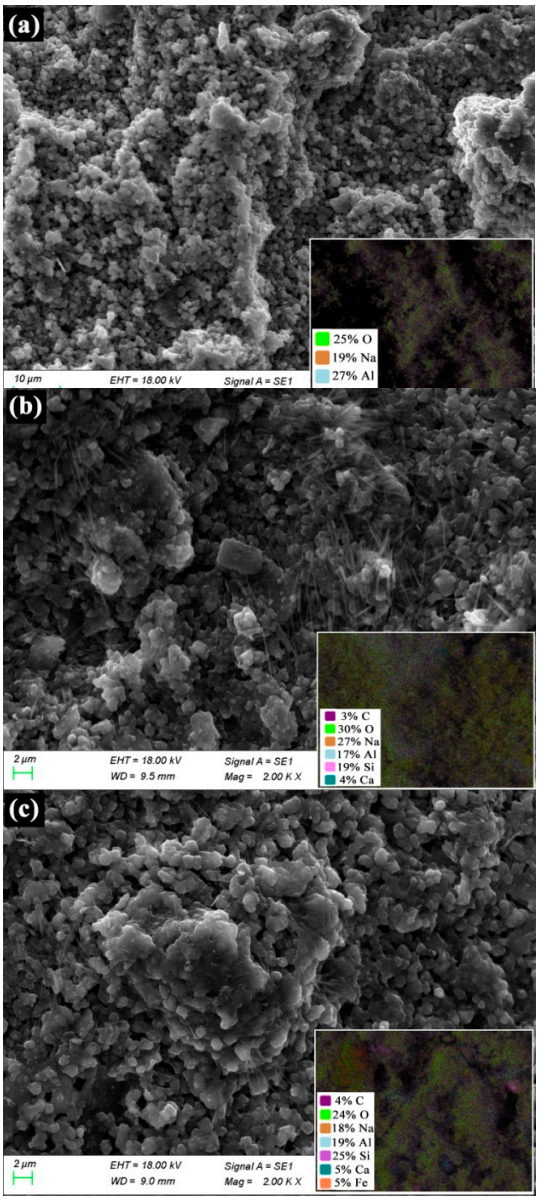

Figure 3. Scanning electron microscopy (SEM)-images for the hydrothermal alkali-activation products of; (**a**) China clay, (**b**) China clay and calcite, and (**c**) calcite-bearing kaolin.

The complete transformation of kaolinite to zeolites in all three specimens was confirmed by their infrared spectra (Figures 4 and 5). The untreated clays produced characteristic infrared bands at 1400–400 cm^{-1} for Si–O, Si–O–Al vibrations, and at 4000–3500 cm^{-1} for the –OH vibration. The conversion to zeolites resulted in the absence of these bands, leaving a sharp band at 945–960 cm^{-1} as the major feature.

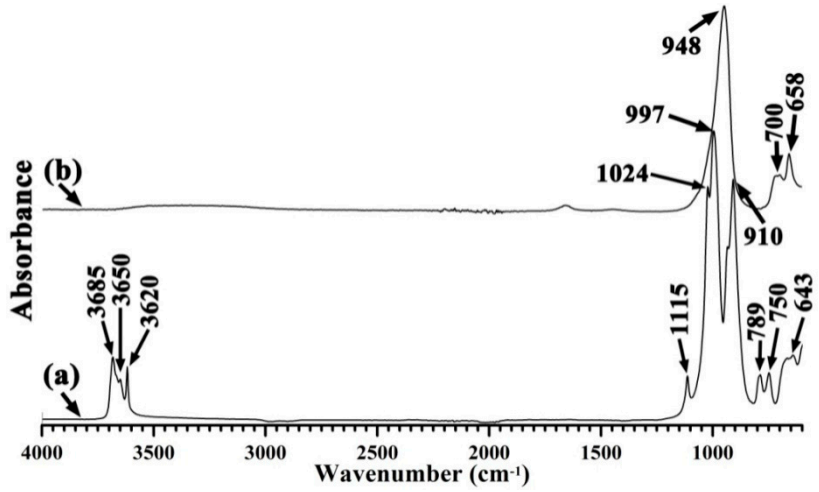

Figure 4. Fourier-transform infrared spectroscopy–attenuated total reflectance (FTIR-ATR) spectra of (**a**) China clay and (**b**) hydrothermal alkali-activation of China clay.

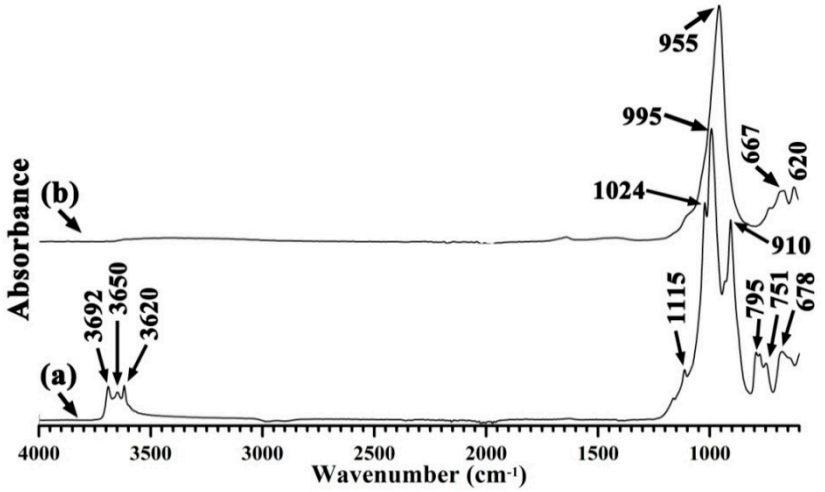

Figure 5. Fourier-transform infrared spectroscopy–attenuated total reflectance (FTIR-ATR) spectra of (**a**) calcite-bearing kaolin and (**b**) hydrothermal alkali-activation of calcite-bearing kaolin.

The nitrogen adsorption-desorption isotherms of the synthesized zeolites are identified as type IVa following the International Union of Pure and Applied Chemistry (IUPAC) classification (Figure 6). This type of physisorption isotherm is characteristic of mesoporous (2–50 nm) adsorbents [43]. It has been reported that the mesoporous structure is favorable for the ion exchange process since it provides more access sites for sorbate cations to approach the inner micropores within the zeolite structure [31]. The specific surface area and porous properties of the synthesized zeolites, presented in Table 3, show the surface area values (BET, DR, and BJH) of the synthesized hydroxy-sodalite to range between 13 and 17 $m^2 \cdot g^{-1}$, whereas the synthesized hydroxy-sodalite/cancrinite composite samples reach values between 16 and 20 $m^2 \cdot g^{-1}$. In contrast, the average pore size of all synthesized zeolites is seen to be similar and ranges from 19 to 21 nm.

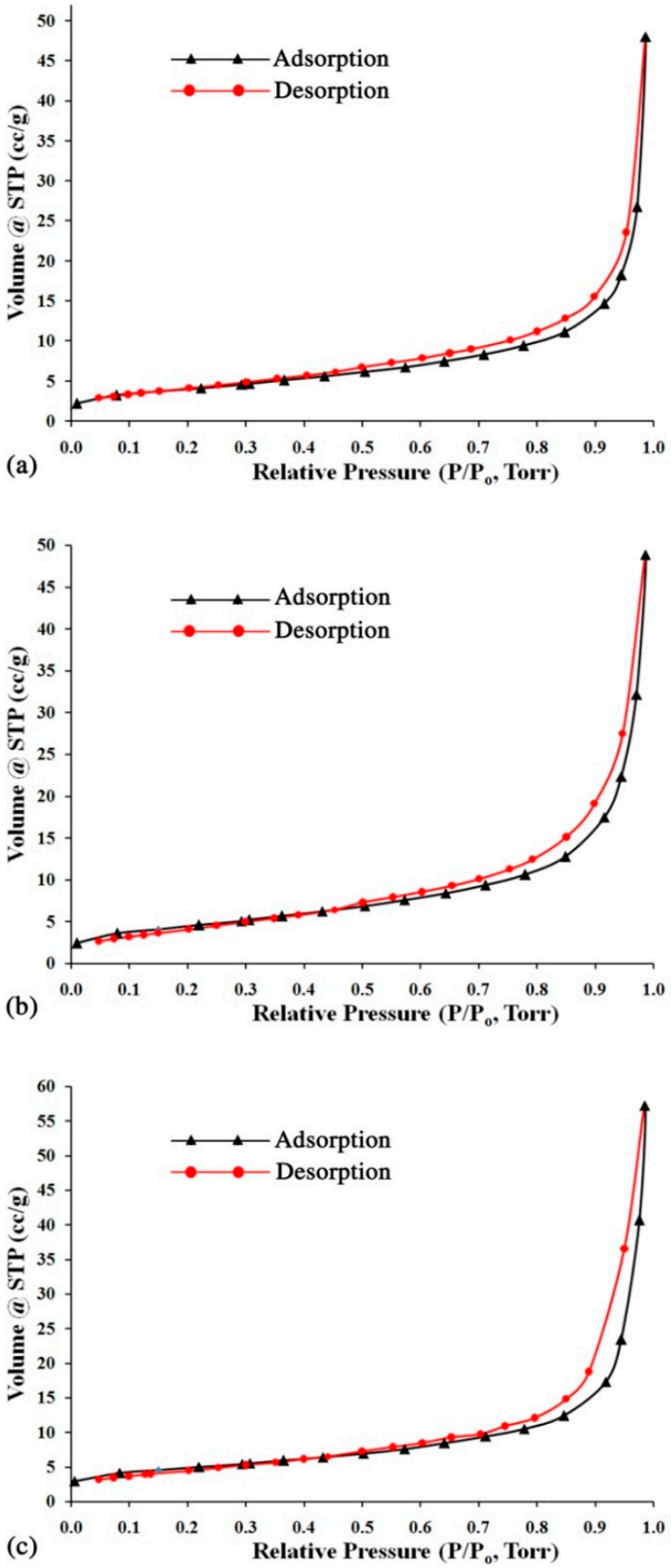

Figure 6. The N_2 adsorption-desorption isotherms for the hydrothermal alkali-activation products of (**a**) China clay, (**b**) China clay and calcite, and (**c**) calcite-bearing kaolin.

Table 3. Surface area and pore-size properties of hydrothermal alkali-activation products.

Sample	S_{BET} [a] ($m^2 \cdot g^{-1}$)	S_{DR} [b] ($m^2 \cdot g^{-1}$)	S_{BJH} [c] ($m^2 \cdot g^{-1}$)	V_{micro} [b] ($m^3 \cdot g^{-1}$)	D_{micro} [b] (nm)	V_{meso} [c] ($m^3 \cdot g^{-1}$)	D_{meso} [c] (nm)
China Clay + NaOH	14.5	17.1	13.1	0.06	2.1	0.07	19.3
China Clay + calcite + NaOH	16.0	18.5	15.4	0.07	2.0	0.07	20.5
Calcite-bearing kaolin + NaOH	16.9	20.2	20.3	0.07	1.8	0.09	21.1

[a] Surface area calculated using the BET equation. [b] Micropore surface area, micropore volume, and average pore diameter calculated by the DR method. [c] Surface area, mesopore volume, and average pore diameter calculated by the BJH method.

3.2. Metal Uptake Behavior of the Synthesized Zeolites

Although sorption isotherms were not determined in this study, the effect of the synthesized composite adsorbent dosage on the removal of heavy metals in single solution systems is shown quantitatively in Figure 7. As expected, the removal efficiencies of heavy metals increased with the higher dosage of both types of synthesized zeolite, which followed the order of $Pb^{2+} > Cu^{2+} > Zn^{2+} > Ni^{2+}$. The better performance of heavy metal removal exhibited by the synthesized zeolite composite for Pb^{2+} over Cu^{2+}, Zn^{2+}, Ni^{2+} may be attributed to the smaller hydrated radius of Pb^{2+} (4.01 Å for Pb, 4.19 Å for Cu, 4.30 Å for Zn, and 4.04 Å for Ni) [47,48]. According to Golomeova et al. [48] cations with smaller ionic or hydration radius adsorbed faster and in larger quantities compared to larger cations, since the smaller cations have more chance to pass through the micropores and channels of the zeolite structure.

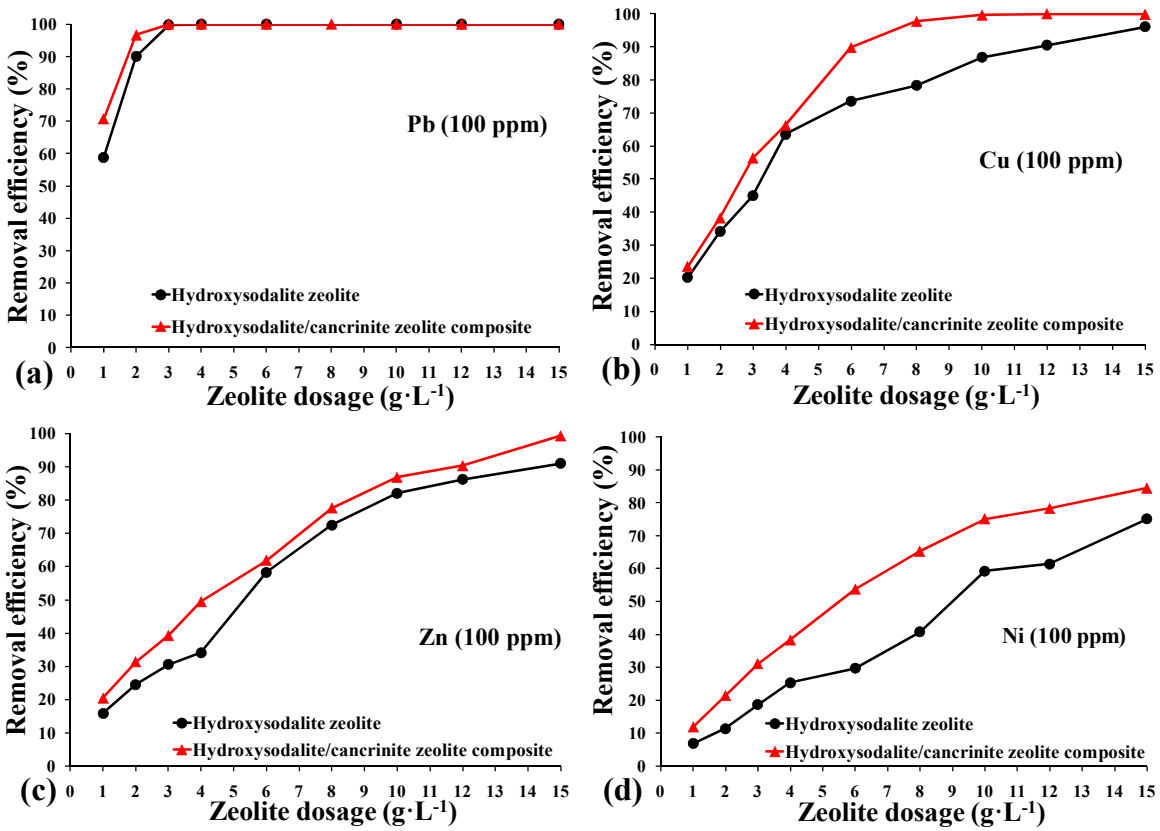

Figure 7. Effect of adsorbent dosage on the removal efficiency of heavy metal ions (100 ppm); (**a**) Pb^{2+}, (**b**) Cu^{2+}, (**c**) Zn^{2+}, and (**d**) Ni^{2+}. (▲) Hydroxy-sodalite zeolite synthesized from China clay, and (●) hydroxy-sodalite/cancrinite zeolite composite synthesized from calcite-bearing kaolin.

As the zeolite dosage was increased from 1 to 6 g L^{-1}, the removal efficiency correspondingly increased from 59% to 99% for Pb^{2+}, 20% to 90% for Cu^{2+}, 16% to 62% for Zn^{2+}, and 7% to 54% for Ni^{2+}. When the zeolite dosage exceeded 12 g·L^{-1}, Pb^{2+} and Cu^{2+} ions were completely removed, together with >90% of the Zn^{2+} and >78% of the Ni^{2+}. The hydroxy-sodalite/cancrinite zeolite composite synthesized from the calcite-bearing kaolin achieved higher removal efficiencies for Cu^{2+} (5%), Zn^{2+} (10%), and Ni^{2+} (10%) when compared to the highest dosage of hydroxy-sodalite synthesized from China clay. The significantly improved removal efficiency of the hydroxy-sodalite/cancrinite composite can be explained by its larger specific surface area, which has a higher adsorption capacity than the single hydroxy-sodalite adsorbent system. These results are comparable to that obtained from zeolites synthesized from fly ash with removal efficiencies of 100% for Pb^{2+}, 95% for Cu^{2+}, and 65% for Ni^{2+} when using a zeolite dosage of 6 g·L^{-1} [49]. In contrast, fly ash showed significantly lower removal efficiency values of 50% for Pb^{2+}, 25% for Cu^{2+}, and 22% for Ni^{2+} when using an equivalent dosage [49].

4. Implications for Water Purification

The hydroxy-sodalite/cancrinite zeolite composite synthesized from calcite-bearing kaolin showed increased heavy metal adsorption compared to the hydroxy-sodalite synthesized from pure kaolinite. Overall, the studied composite achieved a 16–24% improvement in the concentration of heavy metals adsorbed when tested under comparable conditions. The novelty of this work lies in the synthesis of hydroxy-sodalite/cancrinite composite from regionally available Jordanian calcite-bearing kaolin by a cost and energy-efficient production process. As the precursor material used in this study represents a cheap raw commodity that is not used in any industrial applications, the synthesized zeolite composite has the potential to lower the water treatment cost and increase the efficiency of metal removal from aqueous media. The production cost of hydroxy-sodalite/cancrinite composite from calcite-bearing kaolin is estimated to be as low as 2 US$/kg (Table 4), which is 90 times cheaper than the cost of commercial activated carbon (271 US$/kg) [50], 15 times cheaper than the activated carbon produced from waste cherry kernels (42 US$/kg) [50], and 12 times cheaper than Na-A and Na-X zeolite produced from coal fly ash (25 US$/kg) [25]. Further development of adsorbent beds composed of hydroxy-sodalite/cancrinite composites will require adsorption isotherms studies of single and multi-heavy metals solution systems as well as investigations on the role of the adsorbent's particle size.

Table 4. Estimated production costs for 1 kg of hydroxy-sodalite/cancrinite composite.

Materials	Rate in US$/kg	Quantity in kg	Total Cost in US$
Calcite-bearing kaolin [1]	0.13	0.8	0.10
Kaolin grinding and packing cost [1]	0.30	-	0.30
Sodium hydroxide solution (50% wt/wt) [2]	1.0	0.4	0.40
Transportation	0.30	-	0.30
Cost of electric power consumed	0.55	-	0.55
Labor cost	0.35	-	0.35
Total cost/kg of composite			2.0

[1]: Sales price offered by local kaolin mine in Batn El-Ghoul deposit. [2]: Sales price offered by National Chlorine and Soda Industries Company.

5. Conclusions

This study highlights the suitability of a synthetic hydroxy-sodalite/cancrinite zeolite composite obtained from the hydrothermal alkali-activation of regionally available Jordanian calcite-bearing kaolin. The complete dissolution of the calcite-bearing kaolin is accompanied by the formation of a zeolite composite consisting of pseudo-hexagonal hydroxy-sodalite crystals and hexagonal needles of cancrinite. During alkali activation, the kaolinite and quartz act as solid precursor phases that provide the dissolved Al and Si required for zeolite formation, whereas the calcite provides the necessary Ca^{2+} required to form cancrinite. Once the supply of Ca^{2+} is depleted, hydroxy-sodalite forms in a second stage of the reaction. The synthesized zeolite composite exhibits a mesoporous structure with an average pore size of 21 nm, a specific surface area of 20 $m^2 \cdot g^{-1}$, and excellent adsorption capacity. The synthesized zeolite composite acts as a potential adsorbent for the removal of heavy metals from aqueous media. Based on batch experiments, the material effectively removed 99% Pb^{2+}, 90% Cu^{2+}, 62% Zn^{2+}, and 54% Ni^{2+} from a simulated wastewater solution when using a zeolite dosage of 6 $g \cdot L^{-1}$, which is a significantly better performance than documented for fly ash based products tested under equivalent conditions. The use of low-grade calcite-bearing kaolin to synthesize zeolite composites could significantly reduce the production costs of such adsorbents and estimates indicate a price as low as 2 US$ per kg is applicable. Such low regions w-cost adsorbents are particularly relevant to the removal of heavy metals from wastewater in arid here sustainable precursor clays are available in regional proximity.

Author Contributions: M.E. and L.N.W. conceived and designed the experiments; M.E. and L.N.W., writing—original draft preparation; M.E. and L.N.W. writing—review and editing; L.N.W. and G.G. supervised the work and contributed in analyzing of the obtained results; T.M. and M.-T.S. contributed in the heavy metals adsorption experiment; A.K. and H.T. contributed to infrared spectroscopy and nitrogen adsorption/desorption measurements.

Funding: This research was funded by the German Academic Exchange Service (DAAD), 2017 (57299291) and conducted at the University of Greifswald.

Acknowledgments: We acknowledge support for the Article Processing Charge from the DFG (German Research Foundation, 393148499) and the Open Access Publication Fund of the University of Greifswald. The authors are grateful to the staff of Leibniz Institute for Plasma Science and Technology (INP) at Greifswald-Germany for the assistance with ATR-IR and N_2 adsorption/desorption isotherms measurements.

Conflicts of Interest: The authors declare no conflict of interest.

References

1. Abdulla, F.A.; Alfarra, A.; Abu Qdais, H.; Sonneveld, B.G.J.S. Evaluation of wastewater treatment plants in Jordan and suitability for reuse. *Acad. J. Environ. Sci.* **2016**, *4*, 111–117. [CrossRef]
2. Halalsheh, M.; Kassab, G. Policy and the governance framework for wastewater irrigation: Jordanian experience. In *Safe Use of Wastewater in Agriculture*; Hettiarachchi, H., Ardakanian, R., Eds.; Springer: Cham, Switzerland, 2018. [CrossRef]
3. Fu, F.; Wang, Q. Removal of heavy metal ions from wastewaters: A review. *J. Environ. Manag.* **2011**, *92*, 407–418. [CrossRef] [PubMed]
4. Gupta, V.K.; Ali, I.; Saleh, T.A.; Nayak, A.; Agarwal, S. Chemical treatment technologies for waste-water recycling—An overview. *Rsc Adv.* **2012**, *2*, 6380–6388. [CrossRef]
5. Mubarak, N.M.; Sahu, J.N.; Abdullah, E.C.; Jayakumar, N.S. Removal of heavy metals from wastewater using carbon nanotubes. *Sep. Purif. Rev.* **2014**, *43*, 311–338. [CrossRef]
6. Chowdhury, S.; Mazumder, M.J.; Al-Attas, O.; Husain, T. Heavy metals in drinking water: Occurrences, implications, and future needs in developing countries. *Sci. Total Environ.* **2016**, *569*, 476–488. [CrossRef] [PubMed]
7. World Health Organization. Guidelines for Drinking-Water Quality: Incorporating First Addendum. 2017. Available online: http://www.who.int/water_sanitation_health/dwq/gdwq0506.pdf (accessed on 3 April 2018).

8. Jeuland, M. Challenges to wastewater reuse in the Middle East and North Africa. *Middle East Dev. J.* **2015**, *7*, 1–25. [CrossRef]
9. Adam, M.R.; Salleh, N.M.; Othman, M.H.D.; Matsuura, T.; Ali, M.H.; Puteh, M.H.; Jaafar, J. The adsorptive removal of chromium (VI) in aqueous solution by novel natural zeolite based hollow fibre ceramic membrane. *J. Environ. Manag.* **2018**, *224*, 252–262. [CrossRef] [PubMed]
10. Wibowo, E.; Rokhmat, M.; Abdullah, M. Reduction of seawater salinity by natural zeolite (Clinoptilolite): Adsorption isotherms, thermodynamics and kinetics. *Desalination* **2017**, *409*, 146–156. [CrossRef]
11. Huang, H.; Yang, L.; Xue, Q.; Liu, J.; Hou, L.; Ding, L. Removal of ammonium from swine wastewater by zeolite combined with chlorination for regeneration. *J. Environ. Manag.* **2015**, *160*, 333–341. [CrossRef]
12. Ibrahim, K.M.; Khoury, H.N.; Tuffaha, R. Mo and Ni removal from drinking water using zeolitic tuff from Jordan. *Minerals* **2016**, *6*, 116. [CrossRef]
13. Yuna, Z. Review of the natural, modified, and synthetic zeolites for heavy metals removal from wastewater. *Environ. Eng. Sci.* **2016**, *33*, 443–454. [CrossRef]
14. Pavelić, S.K.; Medica, J.S.; Gumbarević, D.; Filošević, A.; Pržulj, N.; Pavelić, K. Critical Review on Zeolite Clinoptilolite Safety and Medical Applications in vivo. *Front. Pharmacol.* **2019**, *9*, 1350. [CrossRef] [PubMed]
15. Rhodes, C.J. Properties and applications of zeolites. *Sci. Prog.* **2010**, *93*, 223–284. [CrossRef] [PubMed]
16. Xue, Z.; Li, Z.; Ma, J.; Bai, X.; Kang, Y.; Hao, W.; Li, R. Effective removal of Mg^{2+} and Ca^{2+} ions by mesoporous LTA zeolite. *Desalination* **2014**, *341*, 10–18. [CrossRef]
17. Zayed, A.M.; Selim, A.Q.; Mohamed, E.A.; Wahed, M.S.A.; Seliem, M.K.; Sillanpää, M. Adsorption characteristics of Na-A zeolites synthesized from Egyptian kaolinite for manganese in aqueous solutions: Response surface modeling and optimization. *Appl. Clay Sci.* **2017**, *140*, 17–24. [CrossRef]
18. Tauanov, Z.; Tsakiridis, P.E.; Mikhalovsky, S.V.; Inglezakis, V.J. Synthetic coal fly ash-derived zeolites doped with silver nanoparticles for mercury (II) removal from water. *J. Environ. Manag.* **2018**, *224*, 164–171. [CrossRef] [PubMed]
19. Belviso, C.; Cavalcante, F.; Di Gennaro, S.; Lettino, A.; Palma, A.; Ragone, P.; Fiore, S. Removal of Mn from aqueous solution using fly ash and its hydrothermal synthetic zeolite. *J. Environ. Manag.* **2014**, *137*, 16–22. [CrossRef] [PubMed]
20. Johnson, E.B.G.; Arshad, S.E. Hydrothermally synthesized zeolites based on kaolinite: A review. *Appl. Clay Sci.* **2014**, *97*, 215–221. [CrossRef]
21. Yue, Y.; Gu, L.; Zhou, Y.; Liu, H.; Yuan, P.; Zhu, H.; Bao, X. Template-free synthesis and catalytic applications of microporous and hierarchical ZSM-5 zeolites from natural aluminosilicate minerals. *Ind. Eng. Chem. Res.* **2017**, *56*, 10069–10077. [CrossRef]
22. Esaifan, M.; Khoury, H.; Aldabsheh, I.; Rahier, H.; Hourani, M.; Wastiels, J. Hydrated lime/potassium carbonate as alkaline activating mixture to produce kaolinitic clay based inorganic polymer. *Appl. Clay Sci.* **2016**, *126*, 278–286. [CrossRef]
23. Ghrib, Y.; Frini-Srasra, N.; Srasra, E.; Martínez-Triguero, J.; Corma, A. Synthesis of cocrystallized USY/ZSM-5 zeolites from kaolin and its use as fluid catalytic cracking catalysts. *Catal. Sci. Technol.* **2018**, *8*, 716–725. [CrossRef]
24. Alkan, M.; Hopa, Ç.; Yilmaz, Z.; Güler, H. The effect of alkali concentration and solid/liquid ratio on the hydrothermal synthesis of zeolite NaA from natural kaolinite. *Microporous Mesoporous Mater.* **2005**, *86*, 176–184. [CrossRef]
25. Panitchakarn, P.; Laosiripojana, N.; Viriya-umpikul, N.; Pavasant, P. Synthesis of high-purity Na-A and Na-X zeolite from coal fly ash. *J. Air Waste Manag. Assoc.* **2014**, *64*, 586–596. [CrossRef] [PubMed]
26. Wdowin, M.; Franus, M.; Panek, R.; Badura, L.; Franus, W. The conversion technology of fly ash into zeolites. *Clean Technol. Environ. Policy* **2014**, *16*, 1217–1223. [CrossRef]
27. Kunecki, P.; Panek, R.; Wdowin, M.; Franus, W. Synthesis of faujasite (FAU) and tschernichite (LTA) type zeolites as a potential direction of the development of lime Class C fly ash. *Int. J. Miner. Process.* **2017**, *166*, 69–78. [CrossRef]
28. Esaifan, M.; Rahier, H.; Barhoum, A.; Khoury, H.; Hourani, M.; Wastiels, J. Development of inorganic polymer by alkali-activation of untreated kaolinitic clay: Reaction stoichiometry, strength and dimensional stability. *Constr. Build. Mater.* **2015**, *91*, 251–259. [CrossRef]
29. Querol, X.; Alastuey, A.; López-Soler, A.; Plana, F.; Andrés, J.M.; Juan, R.; Ruiz, C.R. A fast method for recycling fly ash: Microwave-assisted zeolite synthesis. *Environ. Sci. Technol.* **1997**, *31*, 2527–2533. [CrossRef]

30. Shaqour, F.; Ismeik, M.; Esaifan, M. Alkali activation of natural clay using a Ca $(OH)_2$/Na_2CO_3 alkaline mixture. *Clay Miner.* **2017**, *52*, 485–496. [CrossRef]
31. Qiu, W.; Zheng, Y. Removal of lead, copper, nickel, cobalt, and zinc from water by a cancrinite-type zeolite synthesized from fly ash. *Chem. Eng. J.* **2009**, *145*, 483–488. [CrossRef]
32. Borhade, A.V.; Kshirsagar, T.A.; Dholi, A.G.; Agashe, J.A. Removal of heavy metals Cd^{2+}, Pb^{2+}, and Ni^{2+} from aqueous solutions using synthesized azide cancrinite, Na_8 $[AlSiO_4]_6(N_3)_{2.4}$ $(H_2O)_{4.6}$. *J. Chem. Eng. Data* **2015**, *60*, 586–593. [CrossRef]
33. Hackbarth, K.; Gesing, T.M.; Fechtelkord, M.; Stief, F.; Buhl, J.C. Synthesis and crystal structure of carbonate cancrinite Na_8 $[AlSiO_4]_6CO_3$ $(H_2O)_{3.4}$, grown under low-temperature hydrothermal conditions. *Microporous Mesoporous Mater.* **1999**, *30*, 347–358. [CrossRef]
34. Robson, H. *Verified Synthesis of Zeolitic Materials*; Gulf Professional Publishing: Houston, TX, USA, 2001.
35. Xu, B.; Smith, P.; Wingate, C.; De Silva, L. The effect of calcium and temperature on the transformation of sodalite to cancrinite in Bayer digestion. *Hydrometallurgy* **2010**, *105*, 75–81. [CrossRef]
36. Ahmad, R.; Mirza, A. Facile one pot green synthesis of Chitosan-Iron oxide (CS-Fe_2O_3) nanocomposite: Removal of Pb (II) and Cd (II) from synthetic and industrial wastewater. *J. Clean. Prod.* **2018**, *186*, 342–352. [CrossRef]
37. Ahmad, R.; Mirza, A. Adsorption of Pb (II) and Cu (II) by Alginate-Au-Mica bionanocomposite: Kinetic, isotherm and thermodynamic studies. *Process Saf. Environ. Prot.* **2017**, *109*, 1–10. [CrossRef]
38. Unuabonah, E.I.; Agunbiade, F.O.; Alfred, M.O.; Adewumi, T.A.; Okoli, C.P.; Omorogie, M.O.; Taubert, A. Facile synthesis of new amino-functionalized agrogenic hybrid composite clay adsorbents for phosphate capture and recovery from water. *J. Clean. Prod.* **2017**, *164*, 652–663. [CrossRef]
39. Biswas, B.; Warr, L.N.; Hilder, E.F.; Goswami, N.; Rahman, M.M.; Churchman, J.G.; Vasilev, K.; Pan, G.; Naidu, R. Biocompatible functionalisation of nanoclays for improved environmental remediation. *Chem. Soc. Rev.* **2019**, *48*, 3740–3770. [CrossRef]
40. Yasin, S.; Ghannam, A.; Madanat, M.; Sahawneh, J. Mineral Status and Future Opportunity. Amman, Internal Report: Ministry of Energy and Mineral Resources. Amman, Jordan. 2015. Available online: http://www.memr.gov.jo/EchoBusV3.0/SystemAssets/PDFs/AR/MineralTR/kaolin.pdf (accessed on 12 August 2019).
41. Khoury, H.; El-Sakka, W. Mineralogical and industrial characterization of the BatnEl-Ghoul clay deposits, southern Jordan. *Appl. Clay Sci.* **1986**, *1*, 321–351. [CrossRef]
42. Dietel, J.; Steudel, A.; Warr, L.N.; Emmerich, K. Crystal chemistry of Na-rich rectorite from North Little Rock, Arkansas. *Clay Miner.* **2015**, *50*, 297–306. [CrossRef]
43. Thommes, M.; Kaneko, K.; Neimark, A.V.; Olivier, J.P.; Rodriguez-Reinoso, F.; Rouquerol, J.; Sing, K.S. Physisorption of gases, with special reference to the evaluation of surface area and pore size distribution (IUPAC Technical Report). *Pure Appl. Chem.* **2015**, *87*, 1051–1069. [CrossRef]
44. Zhang, Y.; Dong, J.; Guo, F.; Shao, Z.; Wu, J. Zeolite Synthesized from Coal Fly Ash Produced by a Gasification Process for Ni^{2+} Removal from Water. *Minerals* **2018**, *8*, 116. [CrossRef]
45. Esaifan, M.; Hourani, M.; Khoury, H.; Rahier, H.; Wastiels, J. Synthesis of hydroxysodalite zeolite by alkali-activation of basalt powder rich in calc-plagioclase. *Adv. Powder Technol.* **2017**, *28*, 473–480. [CrossRef]
46. Kriaa, A.; Saad, K.B.; Hamzaoui, A.H. Synthesis and characterization of cancrinite-type zeolite, and its ionic conductivity study by AC impedance analysis. *Russ. J. Phys. Chem. A* **2012**, *86*, 2024–2032. [CrossRef]
47. Nightingale, E.R., Jr. Phenomenological theory of ion solvation. Effective radii of hydrated ions. *J. Phys. Chem.* **1959**, *63*, 1381–1387. [CrossRef]
48. Golomeova, M.; Zendelska, A.; Blažev, K.; Krstev, B.; Golomeov, B. Removal of heavy metals from aqueous solution using clinoptiloliteand stilbite. *Int. J. Eng. Res. Technol.* **2014**, *3*, 1029–1035.
49. He, K.; Chen, Y.; Tang, Z.; Hu, Y. Removal of heavy metal ions from aqueous solution by zeolite synthesized from fly ash. *Environ. Sci. Pollut. Res.* **2016**, *23*, 2778–2788. [CrossRef]
50. Vukelic, D.; Boskovic, N.; Agarski, B.; Radonic, J.; Budak, I.; Pap, S.; Sekulic, M.T. Eco-design of a low-cost adsorbent produced from waste cherry kernels. *J. Clean. Prod.* **2018**, *174*, 1620–1628. [CrossRef]